ACCSCIENCE PUBLISHING

International Journal of Bioprinting

RESEARCH ARTICLE

A vascularized 3D-bioprinted model of the osteosarcoma microenvironment reveals a proliferation-to-invasion switch that confers chemoresistance

Supplementary Files

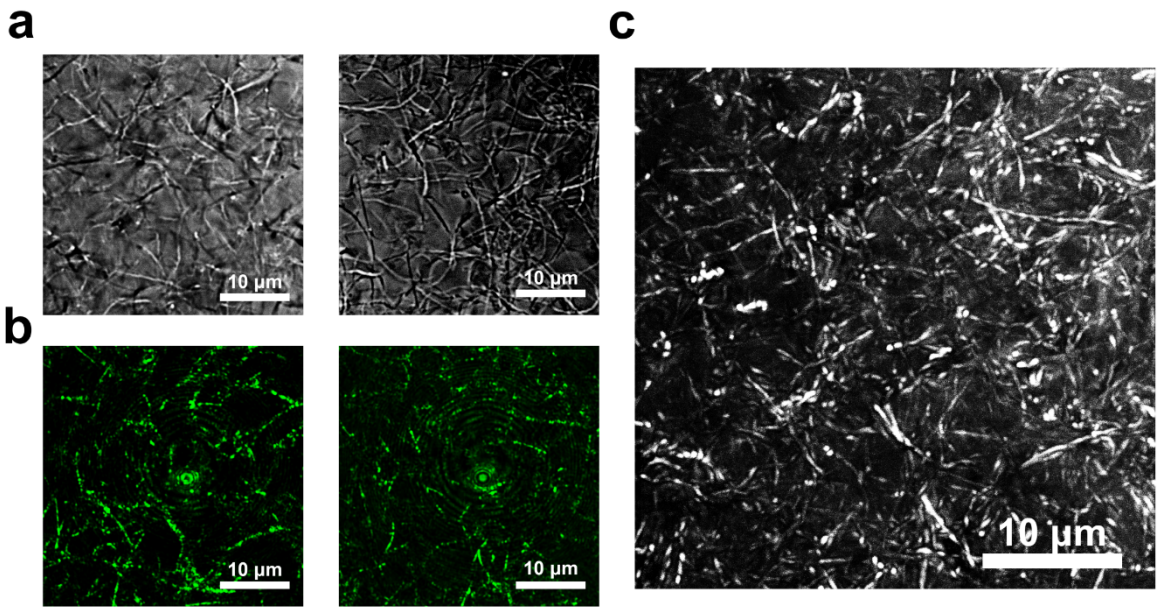

Figure S1. Reflectance confocal imaging of the fibrillar microarchitecture of hydrated type I collagen hydrogels. Hydrated type I collagen hydrogels were imaged in a label-free manner using an Olympus FV3000 laser scanning confocal microscope in reflectance mode. A 488 nm laser was used for excitation, and reflected signals were collected through the reflectance optical pathway within the 480–500 nm detection window to visualize the collagen fibrillar network under fully hydrated conditions. (a) Representative single-plane image acquired using the Transmitted light detector (TD). (b) Representative single-plane image acquired using the High-sensitivity detector (HSD) . Under both acquisition settings, thin filamentous and linear collagen fibers were clearly resolved, forming an interconnected fibrillar network. (c) Maximum intensity projection of a z-stack acquired over a depth of 80 μm, showing the overall three-dimensional organization of the collagen network. The interwoven collagen fibrils formed a continuous hydrogel architecture with abundant pore-like interfibrillar voids. The pinhole was set to 1 Airy unit (1 AU), and the remaining acquisition settings were adjusted to ensure sufficient signal intensity without saturation. Scale bars: 10 μm; magnification: 40×.

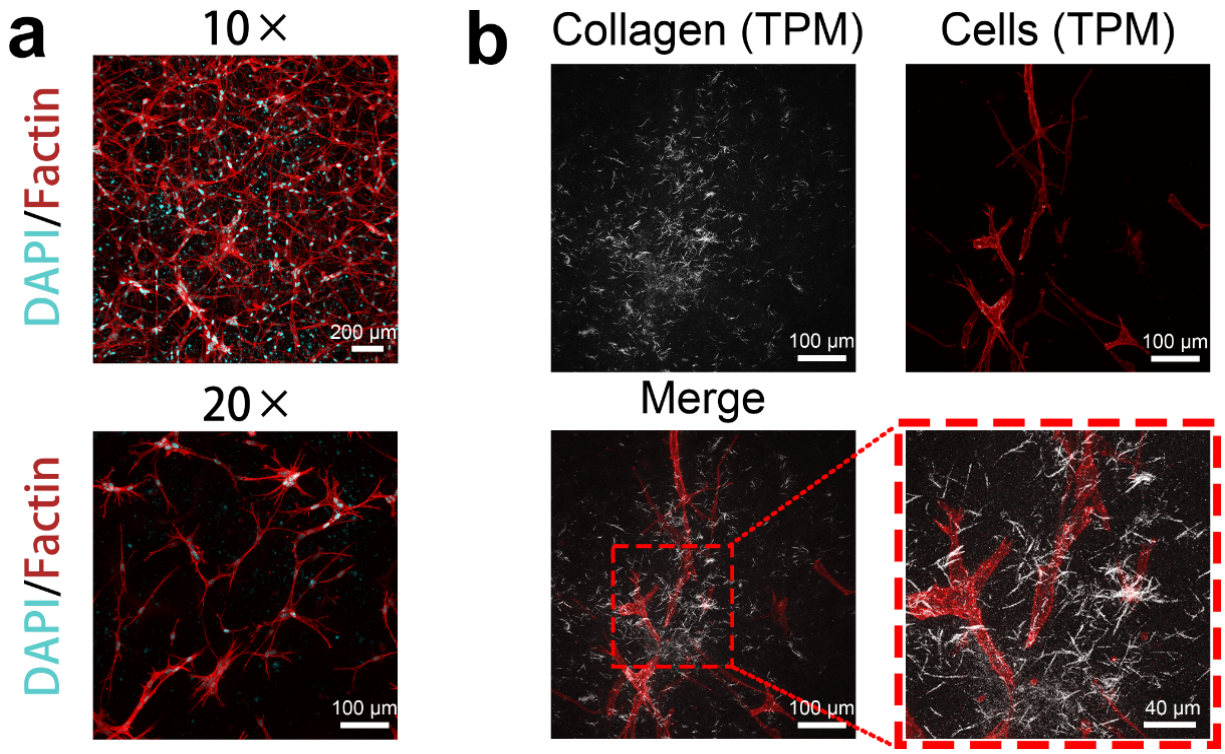

Figure S2. Visualization of cellular morphology and cell–matrix interactions within the 3D-engineered microenvironment. (a) Representative confocal laser scanning microscopy images at 10× and 20× magnification showing cellular morphology and cytoskeletal organization in the engineered microenvironment. Cells were stained for F-actin (red) and nuclei (DAPI, cyan). (b) Representative two-photon microscopy (TPM) images showing the spatial relationship between the collagen matrix (gray) and the cellular network (red). Merged images and enlarged views highlight the close association between cells and the surrounding collagen fibers.

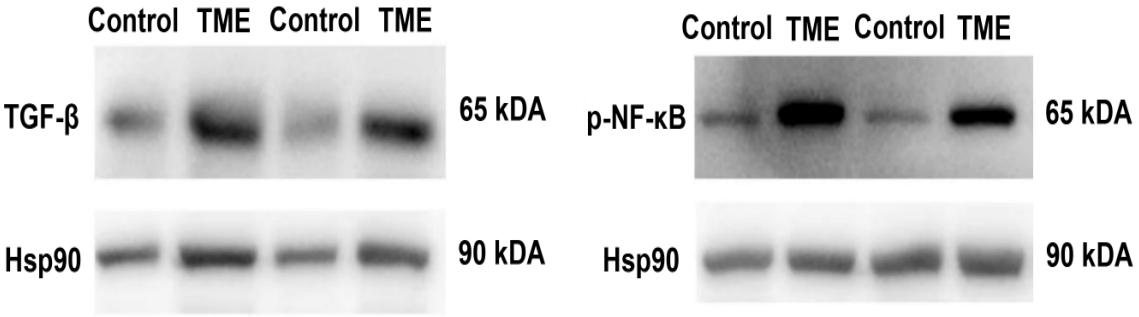

Figure S3. Western blot validation of representative signaling pathways associated with the vascularized tumor microenvironment. Western blot analysis of TGF-β and phosphorylated NF-κB (p-NF-κB) in the control and tumor microenvironment (TME) groups. Compared with the control group, both TGF-β and p-NF-κB showed increased expression in the TME group. Hsp90 was used as the loading control. Representative blots from two of three independent biological replicates are shown.

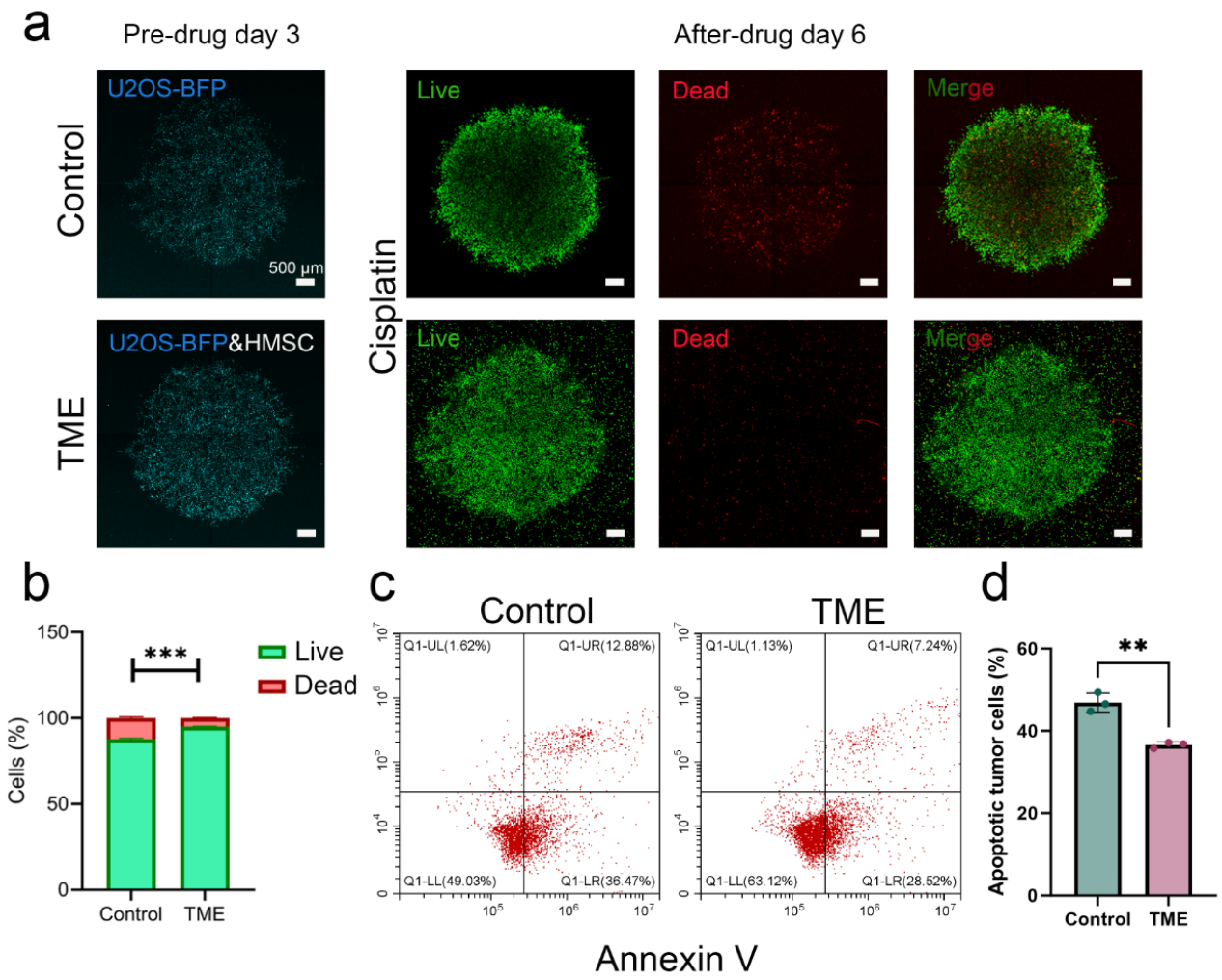

Figure S4. Evaluation of cisplatin response in the 3D-bioprinted tumor microenvironment (TME). (a) Representative fluorescence images showing the morphology of U2OS-BFP tumor spheroids at pre-drug day 3, together with live/dead staining images at day 6 after treatment with 50 μM cisplatin in the control and TME groups. Scale bars: 500 μm; magnification: 4×. (b) Quantitative analysis of the live/dead cell ratio in the control and TME groups after cisplatin treatment. (c) Representative flow cytometry plots of apoptosis (Annexin V & PI) in dissociated tumor cells from the control and TME groups following cisplatin exposure. (d) Quantitative flow cytometric analysis of apoptotic tumor cells in the two groups. Statistical significance was determined by Student's t-tests. Significance levels are indicated as follows: $^{**}p < 0.01$; $^{***}p < 0.001$.

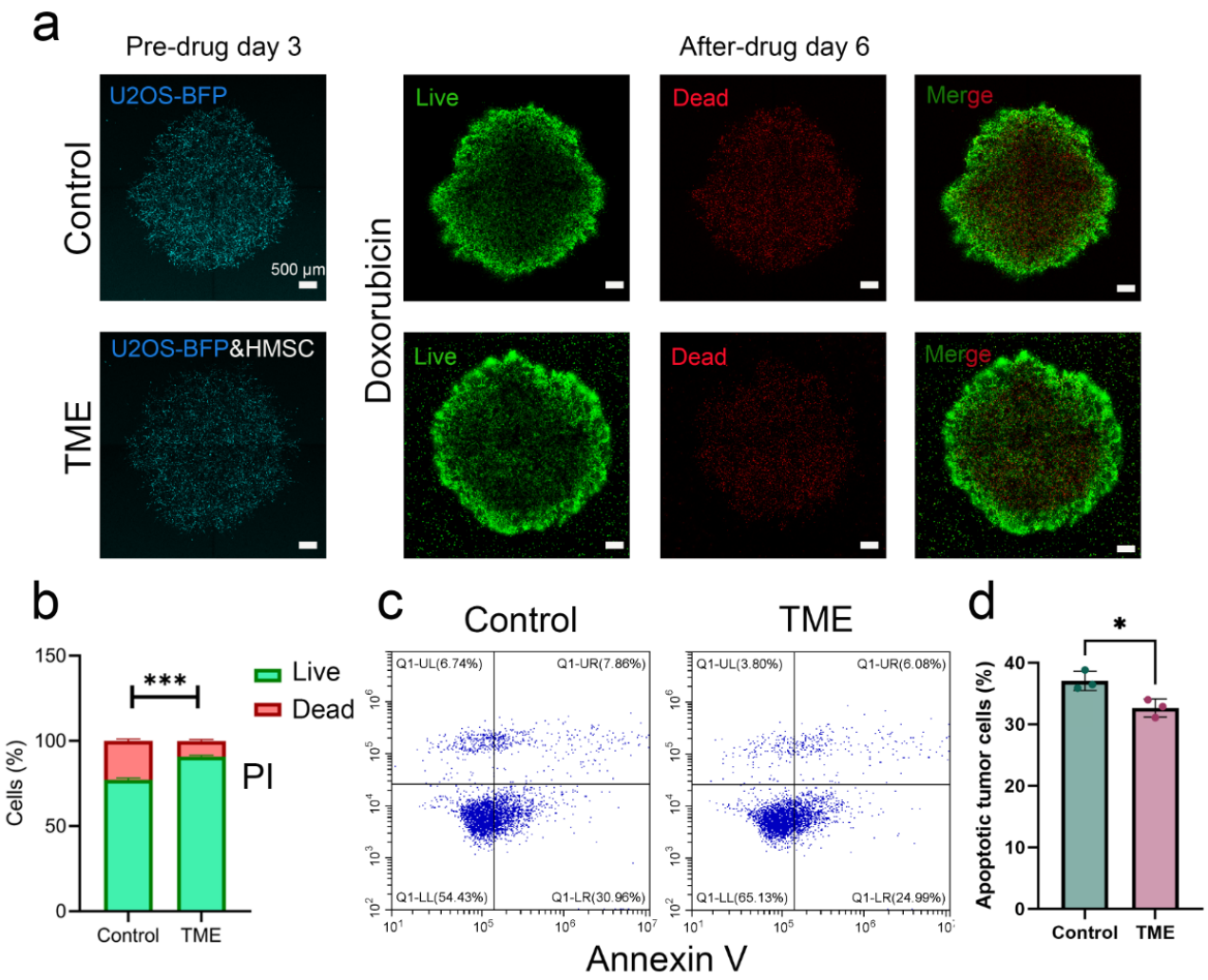

Figure S5. Evaluation of doxorubicin response in the 3D-bioprinted tumor microenvironment (TME). (a) Representative fluorescence images showing the morphology of U2OS-BFP tumor spheroids at pre-drug day 3, together with Live/Dead staining images at day 6 after treatment with 10 μM doxorubicin in the control and TME groups. Scale bars: 500 μm; magnification: 4×. (b) Quantitative analysis of the live/dead cell ratio in the control and TME groups after doxorubicin treatment. (c) Representative flow cytometry plots of apoptosis (Annexin V & PI) in dissociated tumor cells from the control and TME groups following doxorubicin exposure. (d) Quantitative flow cytometric analysis of apoptotic tumor cells in the two groups. Statistical significance was determined by Student's t-tests. Significance levels are indicated as follows: $^{*}p < 0.05$; $^{***}p < 0.001$.